frontiers | Frontiers in Energy Research

TYPE Original Research
PUBLISHED 20 January 2023
DOI 10.3389/fenrg.2022.1084295

OPEN ACCESS

EDITED BY
Lipeng Zhu,
Hunan University, China

REVIEWED BY
Zhengwen Huang,
Brunel University London,
United Kingdom
Izham Zainal Abidin,
Universiti Tenaga Nasional, Malaysia

*CORRESPONDENCE
Zhiyuan Tang,
tangzhiyuan@scu.edu.cn

SPECIALTY SECTION
This article was submitted to Smart Grids, a section of the journal Frontiers in Energy Research

RECEIVED 30 October 2022
ACCEPTED 06 December 2022
PUBLISHED 20 January 2023

CITATION
Liu T, Tang Z, Huang Y, Xu L and Yang Y (2023), Online prediction and control of post-fault transient stability based on PMU measurements and multi-task learning.
Front. Energy Res. 10:1084295.
doi: 10.3389/fenrg.2022.1084295

Online prediction and control of post-fault transient stability based on PMU measurements and multi-task learning

Tingjian Liu[1], Zhiyuan Tang[1]*, Yuan Huang[1], Lixiong Xu[1] and Yue Yang[2]

[1]College of Electrical Engineering, Sichuan University, Chengdu, China, [2]Electric Power Research Institute of Guangdong Power Grid Co. Ltd, Guangzhou, China

The combined usage of phasor measurement units and machine learning algorithms provides the opportunity for developing response-based wide-area system integrity protection scheme against transient instability in power systems. However, only the transient stability status is usually predicted in the literature, which is not enough for real-time decision-making for response-based emergency control. In this paper, an integrated approach is proposed. The GRU-based predictor is firstly proposed for post-disturbance transient stability prediction. On this basis, a multi-task learning framework is proposed for the identification of unstable machines and also the estimation of generation shedding. Case study on the IEEE 39-bus system demonstrates that, apart from the basic task of transient stability prediction, the proposed GRU-based multi-task predictor can predict the grouping of unstable machines correctly. Moreover, based on the estimated amount of generation shedding, the generated remedial control actions can retain the synchronism of the power system.

KEYWORDS

transient stability assessment, unstable machines, emergency control, system integrity protection scheme, phasor measurement units, gated recurrent unit, deep learning, multi-task learning

1 Introduction

Transient stability refers to the ability of power systems to maintain synchronism when subjected to large disturbances (Hatziargyriou et al., 2021). When a power system is at risk of losing the transient stability, if no proper actions are taken, it may cause cascading outages, uncontrolled network splitting, and eventually wide-spread disruption of electricity supply (Andersson et al., 2005). Therefore, maintaining the secure operation of power systems is of great concern to transmission system operators (TSOs). To protect power systems against transient instability, a considerate amount of research efforts has been spent on developing advanced approaches in the field of power engineering.

Online transient stability assessment (TSA) is the first and foremost step for instability prevention as it provides the TSOs with the ability of situation awareness. The

conventional method for TSA is the time-domain simulation (TDS) (Kundur et al., 1994). However, TDS is not capable for real-time stability assessment as solving the high-dimensional differential algebraic equations (DAEs) of an interconnected transmission system is computationally burdensome. Also, TDS cannot provide the information on the stability margin and the countermeasures against the unstable scenarios. To address these two drawbacks of the TDS method, transient energy function (TEF) methods (Pai, 1989), also known as direct methods, have been studied since 1980s. By comparing the kinetic energy at the fault clearing time with the critical energy, the stability status and the energy margin can be assessed without the need of simulating the post-fault trajectories by the TDS. While the critical energy is related with the controlling unstable equivalent point (CUEP) (Chiang, 2011), the CUEP of an ongoing fault contingency is usually hard to identify in real-time manner.

Both the TDS and the TEF are model-driven methods for TSA. With the development of phasor measurement units (PMUs), data-driven methods are considered as the prospective alternative to the model-driven methods. Emergency single machine equivalent (E-SIME) approach (Pavella et al., 2000) attempts to compute the energy margin based on the synchronized PMU measurements. But still, the critical unstable mode should be predicted correctly so as to ensure the accuracy of this approach. The maximal Lyapunov exponent (MLE) is proposed in (Dasgupta et al., 2015) to detect the divergence or convergence of the generator rotor angle trajectories. But the MLE may oscillate from positive and negative values before the disturbed power system settles down, which thus requires a sufficiently long monitoring window to avoid the misclassification of stability status. In recent years, encouraged by the success of artificial intelligence (AI) in the fields such as computer vision and nature language processing, AI-based approaches are gaining more attentions.

Machine learning (ML) algorithms including the decision trees (DTs) (Yang et al., 2017; Cremer et al., 2019), support vector machines (SVMs) (Wang et al., 2016; Hu et al., 2019), neural networks (NNs) (AL-Masri et al., 2013; Zheng et al., 2017), and ensemble predictors (Kamwa et al., 2010; Qiu et al., 2019) have been proposed for power system security assessment. The existing literature on this topic can be sorted into two categories, which are *Pre-disturbance Stability Assessment* and *Post-disturbance Stability Assessment*, depending on whether the post-disturbance measurement is used as the input features. In this paper, post-disturbance stability assessment is studied. At the early stage of the researches on post-disturbance stability assessment, swallow predictors, such as SVMs and single-layer NNs, are used. Considering that the natural characteristics of power system transient stability is highly nonlinear, feature extraction should be performed before developing the predictor for stability assessment. While some literature adopts the wide-area severity indexes as the input features based on the expects' experience (Kamwa et al., 2010; Wang et al., 2016), voltage templates-based (Rajapakse et al., 2010) and Shapelet learning-based (Zhu et al., 2016; Zhu and Hill, 2022) feature extraction schemes are proposed to improve the performance of the stability predictors. The emerging deep learning algorithms can be used for representation learning without the need of feature engineering. In (Yu et al., 2018), the long short-term memory (LSTM)-based recurrent learning algorithm is proposed to develop a time-adaptive transient stability framework. In (Zhu et al., 2020), a convolution neural network (CNN)-based hierarchical learning machine is proposed to learn transient temporal correlations for online TSA.

When the impending instability status is detected, remedial actions, also termed as system integrity protection scheme (SIPS), should be implemented to retore the synchronism of the power system. In (Bhui and Senroy, 2017), a look-up table of modes of disturbance is proposed to assist the online computation of the CUEP and the critical energy for TEF methods. Following the E-SIME framework, the pair-wise relative energy function is proposed in (Gou et al., 2017) to identify the critical unstable mode and to design the emergency generation shedding scheme for transient instability prevention. Although AI-based pre-disturbance stability predictors have been widely studied and employed to develop the integrated preventive control schemes, such as (Xu et al., 2012; Liu et al., 2014; Liu et al., 2020), AI-based approaches for emergency control against post-disturbance transient instability are rarely reported to the best of the authors knowledge. The decision trees are used to trigger the controlled islanding (Senroy, 2006) and the power regulation of HVDC intertie (Gao and Rovnyak, 2011). But these control actions are determined by offline analysis. In (Paul et al., 2020), the LSTM network is also used as the instability detector and then the remedial actions are determined by the continual monitoring of the out-of-step generators based on the individual machine transient energy function.

With the ever-increasing penetration of renewable energies, TSOs are facing with greater challenges in protecting power system. On one hand, it is more difficult to implement preventive control due to the inadequate resources for operating condition regulation. On the other hand, the intermittency of renewable energies will inevitably increase the variation of the real-time operating condition, which also make it more difficult to design the fixed system integrity protection scheme, that is, effective for different scenarios. Therefore, response-based SIPS should be developed to address the above-mentioned challenges. This paper attempts to fill the gap between PMU-based post-disturbance transient stability prediction and AI-driven real-time decision making of emergency generation shedding in order to develop an integrated wide-area protection and control scheme. The gated recurrent unit (GRU)-based RNN is proposed as the base predictor. As is discussed, the decision-making for post-disturbance transient stability includes the

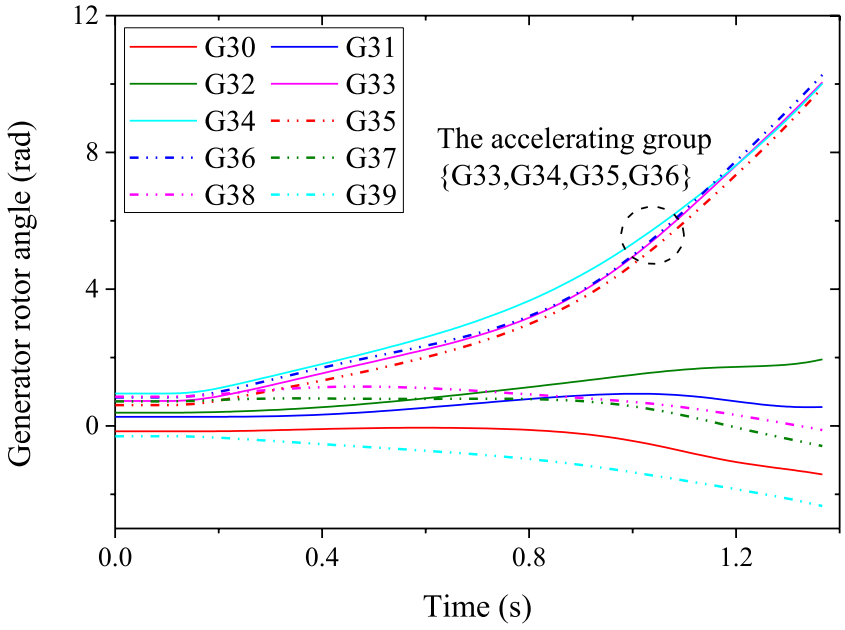

FIGURE 1
The generator rotor angle trajectories under the fault contingency.

prediction of the stability status, the unstable mode and the needed amount of generation shedding. Considering that these three predictive targets are basically correlated tasks, a multi-task learning (MTL) framework is proposed. Case studies on the IEEE 39-bus system is presented to demonstrate the effectiveness of the proposed approach.

The rest of this paper is organized as follows. Problem description is provided in Section 2. The gated recurrent units-based recurrent neural network is introduced in Section 3. The multi-task learning scheme for integrated real-time decision-making of transient stability protection is proposed in Section 4. Case studies on the IEEE 39-bus system is presented to illustrate the effectiveness of the proposed scheme in Section 5. Finally, conclusions are drawn in Section 6.

2 Problem description

As is discussed, transient stability relates to whether the power system can maintain synchronism when subjected to a large disturbance. The disturbance, such as a short-circuit fault, will lead to the imbalance of the mechanical torque and the electrical torque of each of the generators. Then some of the generators will increase their rotor speed with respect to the others, which forms the accelerating group and the decelerating group of generators. The generator rotor angle trajectories under a fault contingency in the IEEE 39-bus system is shown in Figure 1. As can be seen from Figure 1, the generators {G33, G34, G35, G36} together form the accelerating group, while the rest of generators form the decelerating group.

Based on the idea of center of inertia (COI), the accelerating group and the decelerating group of generators can be reduced to two equivalent machines by Eq. 1:

$$\begin{cases} \delta_S = \dfrac{\left(\sum_{i\epsilon S} M_i\delta_i\right)}{M_S, M_S} = \sum_{i\epsilon S} M_i \\ \delta_A = \dfrac{\left(\sum_{j\epsilon A} M_j\delta_j\right)}{M_A, M_A} = \sum_{j\epsilon A} M_j. \end{cases} \tag{1}$$

After the grouping of the generators, the SIngle Machine Equivalent (SIME) can be further determined by Eq. 2:

$$\begin{cases} \delta &= \delta_S - \delta_A \\ M &= \dfrac{M_S M_A}{(M_S + M_A)} \\ \dfrac{d^2\delta}{dt^2} &= M^{-1}(P_m - P_e), \end{cases} \tag{2}$$

where

$$P_m = (M_S + M_A)^{-1}\left(M_A \sum_{i\epsilon S} P_{mi} - M_S \sum_{j\epsilon A} P_{mj}\right), \tag{3}$$

$$P_e = (M_S + M_A)^{-1}\left(M_A \sum_{i\epsilon S} P_{ei} - M_S \sum_{j\epsilon A} P_{ej}\right). \tag{4}$$

After computing the SIME of the multi-machine power system, the conventional equal-area criterion (EAC) can be used to compute the energy margin-based transient stability index (TSI) and to estimate the necessary amount of

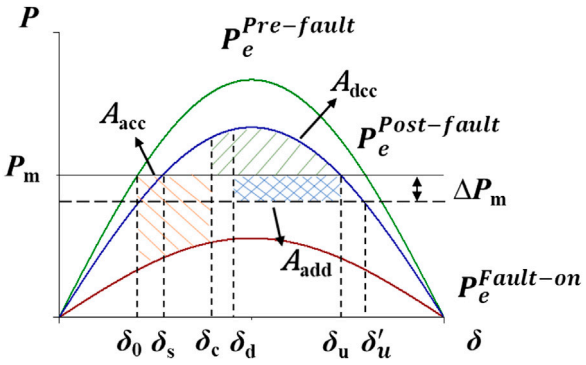

FIGURE 2
Demonstration of generation shedding control based on the EAC criterion.

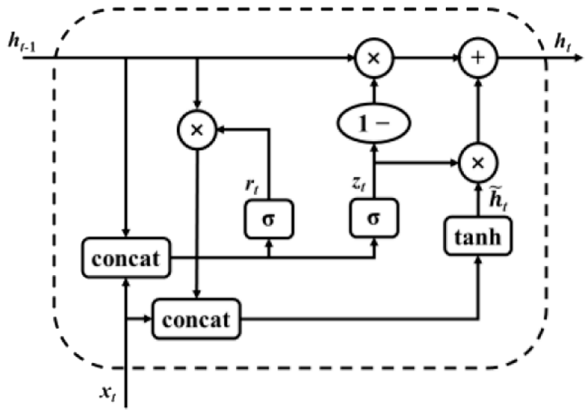

FIGURE 3
The structure of the GRU.

generation shedding for instability prevention when the system is about to lose synchronism. Figure 2 depicts the EAC criterion (Kundur et al., 1994; Gou et al., 2017). If the decelerating area A_{dec} is smaller than the accelerating area A_{acc}, the system will lose synchronism when the operating point travels through the unstable equivalent point (UEP), which refers to the operating point with the equivalent rotor angle to be δ_u.

In Figure 2, δ_0 denotes the rotor angle of the SIME at pre-fault condition, δ_s is the rotor angle relating with the stable equilibrium point of the post-fault condition, while δ_u is the one relating with the unstable equilibrium point of the post-fault condition without generation shedding. δ_c is the rotor angle of the SIME at fault clearing time and δ_d is the rotor angle of the SIME when generation shedding is implemented. Accordingly, $\delta_u^{'}$ is the rotor angle relating with the unstable equilibrium point after generation shedding. Respectively, $P_e^{\text{Pre-fault}}$, $P_e^{\text{Fault-on}}$, and $P_e^{\text{Post-fault}}$ denote the mechanical power output of the SIME for pre-fault condition, fault-on condition and post-fault condition. $\triangle P_{\text{shed}}$ denotes the amount of generation shedding and A_{add} is the increased decelerating area caused by generation shedding.

For unstable cases, generation shedding should be implemented to make the SIME decelerates before travelling through the unstable equivalent point. Based on the EAC, the necessary amount of generation shedding P_{shed} can be computed by Eq. 5 (Pavella et al., 2000; Gou et al., 2017):

$$P_{\text{shed}} = \frac{A_{\text{acc}} - A_{\text{dec}}}{\delta_u^{'} - \delta_d} \approx \frac{E_{KE}(\delta_u)}{\delta_u - \delta_d} = \frac{(1/2)M[\omega(t_u)]^2}{\delta_u - \delta_d}, \quad (5)$$

where $E_{KE}(\delta_u)$ denotes the kinetic energy of the SIME at the UEP. ω is the rotor speed of the SMIE and $\omega(t_u)$ denotes the value at the UEP.

The earlier the control decision is made; the less generation shedding is needed. However, for E-SIME method and its derivatives, it is usually difficult to identify the critical unstable mode and the relative UEP. To tackle this problem, this paper tries to make the best of deep learning algorithms, which have the attractive capability of nonlinear representation and real-time decision-making. By learning from the offline generated knowledge base, the deep learning-based predictor not only predict the stability status, but further address the problems including the grouping of unstable generators and the estimation of the amount of generation shedding.

3 GRU-based RNN for post-fault transient stability prediction

3.1 Brief introduction of gated recurrent unit

As the PMU measurements have the form as temporal sequential data, recurrent neural networks (RNNs) can be used as the predictor for post-fault transient stability assessment. The gated recurrent units (GRU)-based RNN is used in this paper as the base predictor. The structure of the GRU is shown in Figure 3.

GRU consists of the reset gate, the update gate and the state unit. The reset gate $\mathbf{r}_t$ decides whether the previous hidden state $\mathbf{h}_{t-1}$ is ignored and is computed by Eq. 6:

$$\mathbf{r}_t = \sigma\left(\mathbf{W}^{(r)}\mathbf{x}_t + \mathbf{U}^{(r)}\mathbf{h}_{t-1}\right). \quad (6)$$

The update gate $\mathbf{z}_t$ selects whether the hidden state is to be updated and is computed by Eq. 7:

$$\mathbf{z}_t = \sigma\left(\mathbf{W}^{(z)}\mathbf{x}_t + \mathbf{U}^{(z)}\mathbf{h}_{t-1}\right). \quad (7)$$

The actual activation of the state unit $\mathbf{h}_t$ is then computed by Eq. 8:

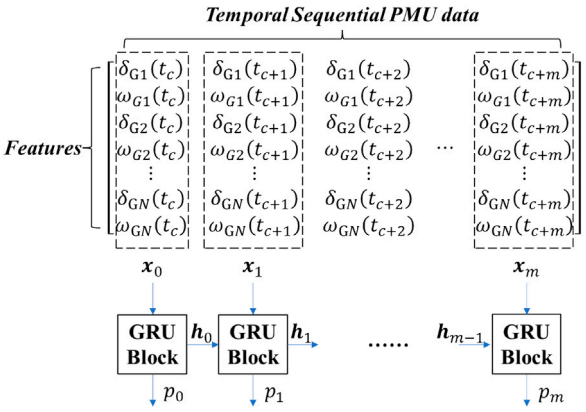

FIGURE 4
The proposed GRU-based transient stability predictor.

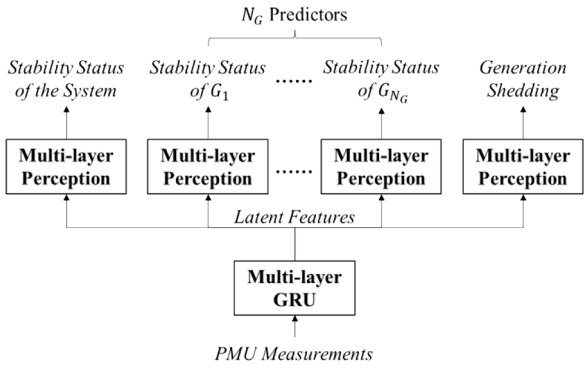

FIGURE 5
The hard parameter sharing structure for transient stability prediction and control.

$$\mathbf{h}_t = \mathbf{z}_t \odot \mathbf{h}_{t-1} + (1 - \mathbf{z}_t) \odot \mathbf{h}_t^{'}, \tag{8}$$

where

$$\mathbf{h}_t^{'} = \tanh\left(\mathbf{W}^{(o)}\mathbf{x}_t + \mathbf{r}_t \odot \mathbf{U}^{(o)}\mathbf{h}_{t-1}\right). \tag{9}$$

In Eqs 6–9, $\mathbf{x}_t$ is the input at current stage. $\odot$ denotes the element-wise product. $\sigma(\cdot)$ and $\tanh(\cdot)$ respectively denote the *sigmoid* activation function and the *tanh* activation function.

3.2 GRU-based post-fault transient stability prediction

The proposed GRU-based transient stability predictor is demonstrated in Figure 4. Assuming that PMUs are equipped at all the generator buses, the rotor angle and the rotor speed of all the generators can be measured by PMUs and then are used as the sequential input for the predictor. Considering the complexity and the nonlinearity of transient stability problem, multi-layer GRU block is used as the predictor. Also, the one-hot encoding is used as the label for post-disturbance transient stability status classification. $y_s = [1, 0]$ indicates that the sample is stable, otherwise, $y_s = [0, 1]$ is referred to as unstable. In this case, the output of the GRU-based predictor is set to be two-dimensional and is preprocessed by *softmax* activation function. With the output of the GRU-based predictor to be $p_s = [p_s(0), p_s(1)]$, following the idea of time-adaptive prediction as in (Yu et al., 2018), decision of transient stability classification is made by Eq. 10:

$$prediction = \begin{cases} Stable, p_s(0) - p_s(1) \geq 0.9 \\ Unstable, p_s(1) - p_s(0) \geq 0.9, \\ Nodecision, otherwise \end{cases} \tag{10}$$

4 Multi-task learning-based framework for transient stability prediction and control

In Section 3, the GRU-based predictor is proposed for post-disturbance transient stability classification. In this section, the predictor is extended for the integrated prediction and control against transient instability by multi-task learning (MTL).

There are a handful of examples of multi-task learning, such as natural language processing (Collobert and Jason, 2008) and computer vision (Girshick, 2015). Although one can handle these tasks in the separated way, i.e., a specific neural network is developed for each task, multi-task learning aims to improve the generalization by leveraging domain-specific information contain in the training signals of related tasks (Ruder, 2017). In practical power systems, there are some transmission interfaces that are correlated in terms of the dominated stability mode. In (Huang et al., 2019), multi-task learning is proposed to train a compact model to evaluate the total transfer capacity (TTC) of these correlated interfaces in the united manner.

The prediction of post-fault stability status, the identification of critical unstable machines, and the estimation of generation shedding are related tasks. Therefore, multi-task learning is used to fulfill the above-mentioned tasks in order to develop the adaptive PMU-based system integrity protection scheme against transient instability. The structure of the multi-task deep neural network is demonstrated in Figure 5. The GRU-based RNN is used to extract the latent features following the basic MTL structure of hard parameter sharing. After extracting the latent features, task-oriented multi-layer perception model are developed to fulfill different tasks. To train the parameters of the multi-task deep neural network, the loss function is defined as is in (11):

$$\mathcal{L} = \mathcal{L}_{TSA} + \sum_{i=1}^{N_G} \mathcal{L}_{Gi} + \mathcal{L}_{GS}, \tag{11}$$

where

$$\mathcal{L}_{TSA} = \frac{1}{N_S} \sum_s -[y_s^{TSA} \log p_s^{TSA} + (1 - y_s^{TSA}) \log p_s^{TSA}], \tag{12}$$

$$\mathcal{L}_{Gi} = \frac{1}{N_S} \sum_s -[y_s^{Gi} \log p_s^{Gi} + (1 - y_s^{Gi}) \log p_s^{Gi}], \tag{13}$$

$$\mathcal{L}_{GS} = \frac{1}{N_S} \sum_s [y_s^{GS} - p_s^{GS}]^2. \tag{14}$$

The subscript s denotes the serial number of a training sample and N_S is the total number of training samples. $\mathcal{L}_{TSA}$ denotes the cross-entropy loss function for transient stability classification. y_s^{TSA} is the label of stability status for the sth sample, while p_s^{TSA} is the related prediction. $\mathcal{L}_{Gi}$ denotes the cross-entropy loss function for the ith generator. y_s^{Gi} is the label that indicates whether the ith generator belongs to the accelerating group for the sth sample, while p_s^{Gi} is the related prediction. $\mathcal{L}_{GS}$ denotes the mean square error (MSE) for generation shedding estimation. y_s^{GS} denotes the amount of generation shedding and is computed by offline SMIE analysis, while p_s^{GS} is the related prediction.

The pseudo-code of the training procedure is demonstrated in Algorithm I.

5 Implementation of the proposed method

The proposed scheme includes two stages, namely the offline model training stage and the online decision-making stage.

5.1 Offline data generation and model training

During the offline stage, data generation is firstly performed. Historical operating conditions (OCs) and stochastic OCs that are simulated by Monte-Carlo sampling of supply and demand are collected to form the database of OCs. For each OC, contingency screening is performed to generate the knowledge base of transient stability. Credible contingencies, including but not limited to N-1 and N-2 fault contingencies, are considered during the generation of knowledge base. The simulated post-disturbance generator rotor angle trajectories are used to simulate the PMU measurements. The stability status is labeled according to whether the maximum separation of rotor angle exceeds 360°. For those unstable instances, the SIME method is used to determine the grouping of unstable generators and the amount of generation shedding. With the generated knowledge base, the multi-task deep neural network is trained and stored for online application.

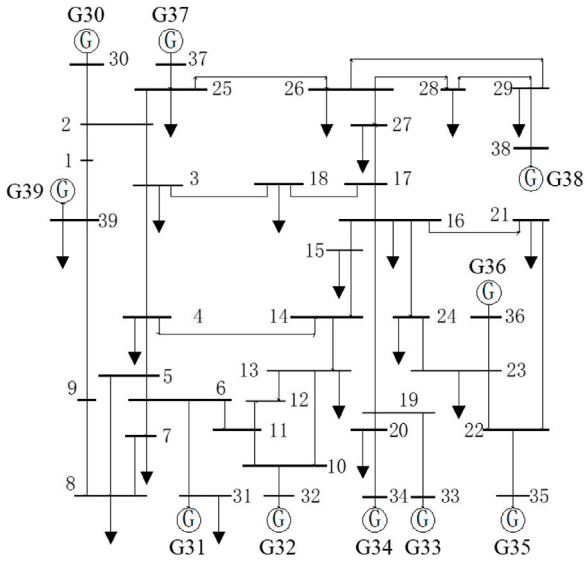

FIGURE 6
The network structure of the testing system.

5.2 Online instability prediction and emergency control

During the online stage, when a fault signal is received, the PMU measurements are collected and are used as the input of the well-trained predictor. The output of transient stability status is checked firstly. If the prediction of stability status is stable, wait for the input of next time step. If the monitoring duration exceed the maximum monitoring window, the protection scheme will disarm and wait for next fault signal. If the prediction of stability status is unstable, the outputs of generator-wise stability status are collected to determine the grouping of accelerating generators. If the unstable mode is multi-machine unstable mode, these unstable generators are ranked according to the output p_s^{Gi}. Then according to the output of generation shedding, the unstable generators are added to the control actions one-by-one until the necessary amount of generation shedding is met by this control action. If the necessary amount of generation shedding is higher than a pre-set threshold, emergency generation shedding may not be the proper countermeasure for transient stability protection. In this case, other measures, such as controlled islanding and load shedding, should be used instead. Otherwise, the generation shedding actions are implemented to retain the synchronism of the disturbed power system.

6 Case studies

The proposed scheme is illustrated by case study on the IEEE 10-machine 39-bus system (Pai, 1989). The network structure of

the testing system is shown in Figure 6. Power flow and time-domain simulation are implemented by using PSD-BPA, which is the power system analysis package developed by the China Electric Power Research Institute (CEPRI). It is assumed that all the generator buses are equipped with PMUs so as to enable post-fault transient stability prediction and real-time decision-making for emergency generation shedding control. Also, all the power plants are assumed to be formed by five identical units that operate in parallel. The maximum number of units that allow to be shed is four so that at least one unit should be connected to the power grid.

6.1 Data generation

Operating conditions of different loading scenarios, which varies from 80% to 120% of base condition with the increment of 5%, are firstly generated. On this basis, the *N*-1 operating scenarios are simulated by randomly selecting one of the transmission lines to be out of service. These normal OCs and *N*-1 OCs are combined to form the database of OCs. Three-phase short-circuit faults, which are isolated by opening the relative transmission line, are considered as credible contingencies. Fault location is randomly chosen at 0%, 50% and 100% of the length of the transmission line, while the fault clearing time is randomly set between 6 cycles and 9 cycles. 5000 samples are generated. For performance evaluation, the samples are separated by 60:20:20, which are then used as the training set, the validation set, and the testing set of samples.

6.2 Development of GRU-based predictor

After knowledge base generation, the GRU-based predictor is trained based on the MTL-based framework proposed in Section 4. As is proposed, the post-disturbance PMU measurements of generator rotor angles and rotor speeds are used as the input features. The hyperparameters of the predictor is determined by trial and error. In this case study, the GRU block consists of two layers and the number of hidden states is set to be 1024. The MLP blocks for all the predicting tasks consists of two hidden layers and the number of hidden states is also set to be 1024. The training epoch is set to be 200, while early stopping is enabled by using the validation data.

6.3 Performance on post-disturbance transient stability assessment

The performance of the well-trained predictor on post-disturbance transient stability assessment is evaluated by using the testing data. The maximum monitoring window is set as six cycles after fault clearing. Two cases, which are fixed-time prediction and time-adaptive prediction, are studied.

1) Fixed-time prediction

In the first case, the post-disturbance PMU measurements from the fault clearing time to the end of the maximum monitoring window are collected and used as the input of the predictor. Numerical results of the confusion matrix in transient stability classification are shown in Table 1. The overall classification accuracy is 99.4%.

2) Time-adaptive prediction

In the second case, the performance of the time-adaptive prediction scheme proposed in Section 3.2 is validated. The testing results of time-adaptive prediction is shown in Table 2. The overall classification accuracy is 99.6%, which is comparable to fixed-time prediction. However, 29.8% of unstable instances can be assessed in three cycles after fault clearing, which helps to enable faster response for remedial control against the impending instability of the power system.

3) Comparison with the task-separated predictor

To demonstrate the effectiveness of the proposed MTL framework, the comparison between the MTL-based predictor and the task-separated predictor is studied. The numerical results are shown in Table 3. False alarm (FA) refers to the ratio of stable cases that are misclassified as unstable, while false dismissal (FD) refers to the ratio of unstable cases that are misclassified as stable. As can be seen from Table 3, the proposed MTL-based predictor achieves higher accuracy in transient stability classification comparing with the separated predictor, that is, trained without the consideration of related tasks. As transient instability will lead to catastrophic blackout, lower value of false dismissal is preferred. In this regard, the proposed MTL-based predictor also performs better that the task-separated predictor.

Apart from post-disturbance transient stability classification, the MTL-based predictor is used for real-time decision-making for mitigation of the impending transient instability. A thorough test on the performance on instability mitigation is investigated. Numerical results are shown in Table 4. There are 357 unstable testing instances. All these unstable instances are correctly classified as unstable. Based on the decision-making scheme proposed in Section 5.2, 337 instances are stabilized by implementing the generated

TABLE 1 The confusion matrix in transient stability classification for fixed-time (6 cycles) prediction.

		Prediction of the testing data	
		Classified as Stable	*Classified as Unstable*
Stability Status of the Testing data	*Stable*	638/643 (99.22%)	5/643 (0.78%)
	Unstable	1/357 (0.28%)	356/357 (99.72%)

TABLE 2 The testing results of time-adaptive prediction in transient stability classification.

Decision-making time (cycles)	Instances to be classified	Instances with classification decision	Correct	Incorrect
3	1000	298	298	0
4	702	22	22	0
5	680	11	11	0
6	669	669	665	4

TABLE 3 Comparison between the MTL-based predictor and the task-separated predictor.

Metrics	MTL-based predictor (%)	Task-separated predictor (%)
Accuracy	99.6	98.8
False Alarm	0.62	0.16
False Dismissal	0.00	3.18

Performance on Real-time Decision-making for Instability Mitigation.

TABLE 4 Numerical results on real-time decision-making for instability mitigation.

Number of unstable testing instances	Instances that are correctly predicted	Instances that are stabilized
357	357(100.0%)	337 (94.4%)

remedial actions. So, the overall percentage of success decision-making is 94.40%.

The procedure of decision-making against transient instability is demonstrated by an unstable testing instance. The rotor angle trajectories without any control actions are shown previously in Figure 1. In this case, the unstable status is predicted at three cycles. After stability prediction, unstable machine identification is enabled by the outputs p_s^{Gi} of the MTL-based predictor. Numerical results are shown in Figure 7 and accordingly the generators (G33, G34, G35, G36) are identified as unstable machines. Then the estimated amount of generation shedding is 558.96 MW. To meet this requirement of generation shedding, 4 units at Bus-36 and 1 unit at Bus-35 are disconnected from the power grid. The power angle trajectories after the control actions are shown in Figure 8. As can be seen from Figure 8, after disconnecting the above-mentioned units, the rest of generators can restore synchronism and the impending instability is mitigated.

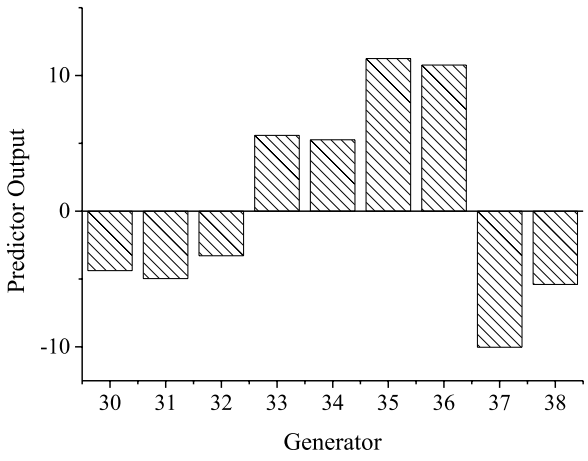

FIGURE 7
Indicator of critical unstable machine based on the output of the MTL predictor.

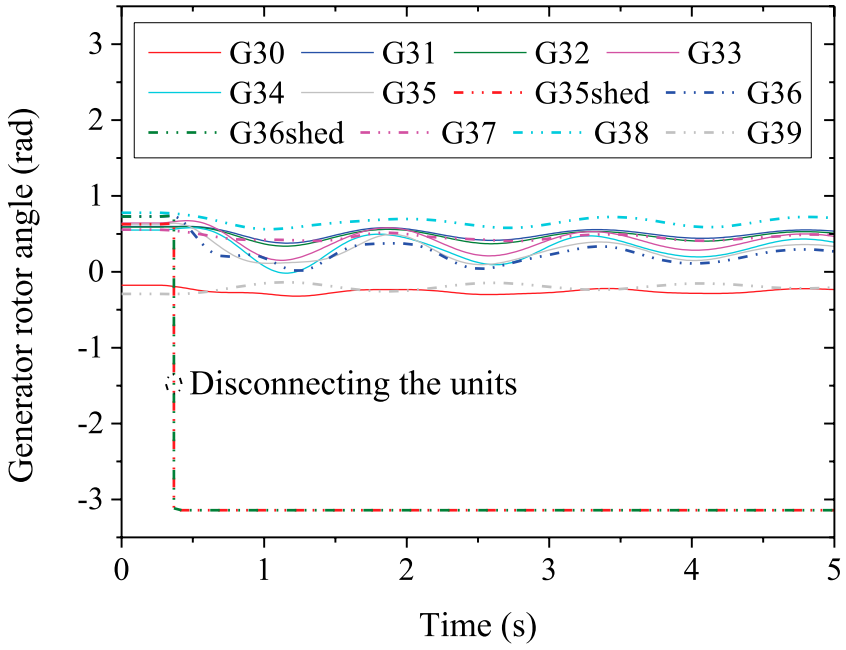

FIGURE 8
The generator rotor angle trajectories after generation shedding control.

7 Conclusion

To protect power systems from transient instability and the subsequent catastrophic blackouts, an integrated scheme is proposed by using post-disturbance PMU measurements and multi-task deep learning. The GRU-based predictor is firstly proposed for post-disturbance transient stability prediction. On this basis, considering that the prediction of the impending instability, the identification of the unstable mode, and the estimation of generation shedding are essentially related tasks, a multi-task learning framework is proposed to develop the PMU-based system integrity protection scheme for transient stability. Case study on the IEEE 39-bus system demonstrates that, apart from the basic task of transient stability prediction, the proposed multi-task predictor can predict the grouping of generators correctly. Moreover, based on the estimated amount of generation shedding, the generated remedial control actions can retain the synchronism of the power system.

Future research involves two aspects:

1) The proposed scheme is an open-loop SIPS and the overall percentage of success decision-making is 94.40% in the case study on the IEEE 39-bus system. In this regard, future research focuses on developing the close-loop SIPS following this paper so as to further enhance the percentage of success decision-making.

2) In this paper, generation shedding of synchronous generators is used as remedial actions. With the increasing penetration of renewables, how to coordinate the conventional generation shedding with the fast regulation of inverter-based renewables is another topic for future work.

Data availability statement

The original contributions presented in the study are included in the article/supplementary material, further inquiries can be directed to the corresponding author.

Author contributions

TL: Methodology, Writing. ZT: Conceptualization, Supervision. YH: Investigation. LX: Software, Validation. YY: Software, Validation.

Funding

This research was supported by “the Fundamental Research Funds for the Central Universities” (Grant no: YJ2021163).

Conflict of interest

YY was employed by the company Electric Power Research Institute of Guangdong Power Grid Co. Ltd.

The remaining authors declare that the research was conducted in the absence of any commercial or financial relationships that could be construed as a potential conflict of interest.

Publisher's note

References

Al-Masri, A. N., Ab Kadir, M. Z. A., Hizam, H., and Mariun, N. (2013). A novel implementation for generator rotor angle stability prediction using an adaptive artificial neural network application for dynamic security assessment. *IEEE Trans. Power Syst* 28 (3), 2516–2525. doi:10.1109/TPWRS.2013.2247069

Andersson, G., Donalek, P., Farmer, R., Hatziargyriou, N., Kamwa, I., and Kundur, P., (2005). Causes of the 2003 major grid blackouts in North America and Europe, and recommended means to improve system dynamic performance. *IEEE Trans. Power Syst* 20 (4), 1922–1928, Nov. doi:10.1109/TPWRS.2005.857942

Bhui, P., and Senroy, N. (2017). Real-time prediction and control of transient stability using transient energy function. *IEEE Trans. Power Syst* 32 (2), 1–934. doi:10.1109/TPWRS.2016.2564444

Chiang, H.-D. (2011). "Controlling UEP method: Theory," in *Direct methods for stability analysis of electric power systems: Theoretical foundation, BCU methodologies, and applications* (IEEE), New York, NY, USA, 177–195. doi:10.1002/9780470872130.ch11

Collobert, R., and Jason, W. (2008). A unified architecture for natural language processing: Deep neural networks with multitask learning. Proceedings of the 25th international conference on Machine learning, Helsinki, Finland, 160–167.

Cremer, J. L., Konstantelos, I., and Strbac, G. (2019). From optimization-based machine learning to interpretable security rules for operation. *IEEE Trans. Power Syst* 34 (5), 3826–3836. doi:10.1109/TPWRS.2019.2911598

Dasgupta, S., Paramasivam, M., Vaidya, U., and Ajjarapu, V. (2015). PMU-based model-free approach for real-time rotor angle monitoring. *IEEE Trans. Power Syst* 30 (5), 2818–2819. doi:10.1109/TPWRS.2014.2357212

Gao, Q., and Rovnyak, S. M. (2011). Decision trees using synchronized phasor measurements for wide-area response-based control. *IEEE Trans. Power Syst* 26 (2), 855–861. doi:10.1109/TPWRS.2010.2067229

Girshick, R. (2015). Fast R-CNN. Proceedings of the IEEE international conference on computer vision, Washington, DC, USA, 1440–1448.

Gou, J., Liu, Y., Liu, J., Taylor, G. A., and Alamuti, M. M. (2017). Novel pair-wise relative energy function for transient stability analysis and real-time emergency control. *IET Gener. Transm. &amp. Distrib* 11 (18), 4565–4575. doi:10.1049/iet-gtd.2016.1671

Hatziargyriou, N., Milanovic, J., Rahmann, C., Ajjarapu, V., Canizares, C., and Erlich, I., (2021). Definition and classification of power system stability – revisited & extended. *IEEE Trans. Power Syst* 36 (4), 3271–3281. doi:10.1109/TPWRS.2020.3041774

Hu, W., Lu, Z., Wu, S., Zhang, W., Dong, Y., and Yu, R., (2019). Real-time transient stability assessment in power system based on improved SVM. *J. Mod. Power Syst. Clean. Energy* 7 (1), 26–37. doi:10.1007/s40565-018-0453-x

Huang, T., Guo, Q., Sun, H., Tan, C.-W., and Hu, T. (2019). A deep learning approach for power system knowledge discovery based on multitask learning. *IET Gener. Transm. &amp. Distrib* 13 (5), 733–740. doi:10.1049/iet-gtd.2018.5078

Kamwa, I., Samantaray, S. R., and Joos, G. (2010). Catastrophe predictors from ensemble decision-tree learning of wide-area severity indices. *IEEE Trans. Smart Grid* 1 (2), 144–158. doi:10.1109/TSG.2010.2052935

Kundur, P., Balu, N. J., and Lauby, M. G. (1994). *Power System Stability And Control*. New York, NY, USA: McGraw-Hill.

Liu, C., Sun, K., Rather, Z. H., Chen, Z., Bak, C. L., and Thogersen, P., (2014). A systematic approach for dynamic security assessment and the corresponding preventive control scheme based on decision trees. *IEEE Trans. Power Syst* 29 (2), 717–730. doi:10.1109/TPWRS.2013.2283064

Liu, T., Liu, Y., Liu, J., Wang, L., Xu, L., and Qiu, G., (2020). A bayesian learning based scheme for online dynamic security assessment and preventive control. *IEEE Trans. Power Syst* 35 (5), 4088–4099. doi:10.1109/TPWRS.2020.2983477

Pai, M. A. (1989). *Energy Function Analysis For Power System Stability*. Boston, MA: Kluwer.

Paul, A., Kamwa, I., and Joos, G. (2020). PMU signals responses-based RAS for instability mitigation through on-the fly identification and shedding of the run-away generators. *IEEE Trans. Power Syst* 35 (3), 1707–1717. doi:10.1109/TPWRS.2019.2926243

Pavella, M., Ernst, D., and Ruiz-Vega, D. (2000). *Transient Stability Of Power Systems: A Unified Approach To Assessment And Control*. Norwell, MA, USA: Kluwer.

Qiu, G., Liu, J., Liu, Y., Liu, T., and Mu, G. (2019). Ensemble learning for power systems TTC prediction with wind farms. *IEEE Access* 7, 16572–16583. doi:10.1109/ACCESS.2019.2896198

Rajapakse, A. D., Gomez, F., Nanayakkara, K., Crossley, P. A., and Terzija, V. V. (2010). Rotor angle instability prediction using post-disturbance voltage trajectories. *IEEE Trans. Power Syst* 25 (2), 947–956. doi:10.1109/TPWRS.2009.2036265

Ruder, S. "An overview of multi-task learning in deep neural networks." arXiv preprint arXiv:1706.05098 (2017).

Senroy, N., and (2006). Decision tree assisted controlled islanding. *IEEE Trans. Power Syst.* 21 (4), 1790–1797, Nov. doi:10.1109/TPWRS.2006.882470

Wang, B., Fang, B., Wang, Y., Liu, H., and Liu, Y. (2016). Power system transient stability assessment based on big data and the core vector machine. *IEEE Trans. Smart Grid* 7 (5), 2561–2570. doi:10.1109/TSG.2016.2549063

Xu, Y., Dong, Z. Y., Guan, L., Zhang, R., Wong, K. P., and Luo, F. (2012). Preventive dynamic security control of power systems based on pattern discovery technique. *IEEE Trans. Power Syst* 27 (3), 1236–1244. doi:10.1109/TPWRS.2012.2183898

Yang, Y., Huang, Y., Liu, J., Liu, Y., Liu, T., and Xiang, Y. (2017). Measurement-based cell-DT method for power system transient stability classification. *CSEE J. Power Energy Syst* 3 (3), 278–285. doi:10.17775/CSEEJPES.2015.01230

Yu, J. J. Q., Hill, D. J., Lam, A. Y. S., Gu, J., and Li, V. O. K. (2018). Intelligent time-adaptive transient stability assessment system. *IEEE Trans. Power Syst* 33 (1), 1049–1058. doi:10.1109/TPWRS.2017.2707501

Zheng, L., Hu, W., Zhou, Y., Min, Y., Xu, X., Wang, C., et al. (2017). *Deep Belief Network Based Nonlinear Representation Learning For Transient Stability Assessment*. Chicago, IL, USA: IEEE Power & Energy Society General Meeting, 1–5. doi:10.1109/PESGM.2017.8274126

Zhu, L., Hill, D. J., and Lu, C. (2020). Hierarchical deep learning machine for power system online transient stability prediction. *IEEE Trans. Power Syst* 35 (3), 2399–2411. doi:10.1109/TPWRS.2019.2957377

Zhu, L., and Hill, D. J. (2022). Networked time series shapelet learning for power system transient stability assessment. *IEEE Trans. Power Syst* 37 (1), 416–428. doi:10.1109/TPWRS.2021.3093423

Zhu, L., Lu, C., and Sun, Y. (2016). Time series shapelet classification based online short-term voltage stability assessment. *IEEE Trans. Power Syst* 31 (2), 1430–1439. doi:10.1109/TPWRS.2015.2413895